15TH IEA HEAT PUMP CONFERENCE
MAY 26–29, 2026 | HOFBURG
VIENNA 2026
DECARBONISATION THROUGH INNOVATION

Control strategy design for large-scale heat pumps: An economic-oriented analysis

Fabrizia Giordano[a,*], Nándor Mihály[a], Thomas Natiesta[a], Bernd Windholz[a], Andreas Fischer[a], Regina Hemm[a], Franziska Zimmer[b] and Ahmed A. Serageldin[a]

[a] AIT Austrian Institute of Technology GmbH, Center for Energy, Giefinggasse 2, 1210 Vienna, Austria
[b] Austrian Energy Agency, Mariahilfer Straße 136, 1150 Vienna, Austria

Abstract

Heat pumps are a central, well-established technology to decarbonize the energy system. Coupled with intelligent control strategies and thermal storage, they can align heat demand with renewable energy generation through load shifting, thereby enhancing both system flexibility and grid stability. This study investigates the impact of different rule-based control strategies for large-scale heat pumps in residential buildings, focusing on their response to fluctuating renewable energy production, variable electricity prices, and grid signals. Simulations of a representative multi-family house model with a centralized 60 kW heat pump are conducted across four control scenarios. The building's thermal mass is modelled as thermal storage and preheated to shift electricity consumption out of periods of high electricity prices. The overarching objective is to reduce operational costs for the user. To achieve this, a simple "Base-case" Scenario (A), including possibility to consume and sell self-produced PV electricity, is compared with three alternative strategies: Scenario (B) "Photovoltaic-induced overconsumption", where economic profitability arises by increased consumption of PV self-produced electricity; Scenario (C) "Variable electricity price", where the heat pump load is positively shifted in response to negative electricity prices; Scenario (D) "Interruptible tariffs", where profit margins are a direct consequence of incentivized reductions in grid tariffs. Results indicate that Scenario (D) achieves the most significant operational cost savings (10.7% OPEX reduction compared to base-case), driven by the reduced grid fees, while maintaining thermal comfort >99.7% of the times. However, the economic benefit comes at the expense of the system performance, with a COP reduction of 6.9% compared to the base-case.

© HPC2026.
Selection and/or peer-review under the responsibility of the organizers of the 15th IEA Heat Pump Conference 2026.

Keywords: Heat pump, control, OPEX, flexibility, efficiency, thermal comfort

1. Introduction

The heating sector is central to Europe's energy transition, accounting for nearly half of final energy demand in buildings and a substantial share of CO_2 emissions [1]. Its decarbonisation is closely tied to the increasing integration of Renewable Energy Sources (RES) within the energy mix. However, the intermittent nature of energy generation from RES necessitates enhanced energy-management strategies and flexibility to ensure the optimal match between energy production and consumption. Specifically, locally generated energy from sources such as photovoltaic (PV) systems determines bi-directional energy flows [2] between buildings entities – now acting as prosumers, e.g. able to generate, consume and sell energy for economic profit [3] – and the grid. In this regard, the recent growth of Renewable Energy Communities (RECs) at European level highlights the increasing need for the development of technical solutions and intelligent energy-management systems to prevent grid congestion issues [4,5]. This dynamic has considerable implications for the distribution

* Corresponding author. Tel.: +43 664 88335463
E-mail address: fabrizia.giordano@ait.ac.at

15th IEA Heat Pump Conference 2026 - FLE1.5 - https://doi.org/10.23697/smeq-ev52

network, as fluctuations in renewable energy supply and feed-in can lead to voltage irregularities, overloads of transmission lines and transformers, and technical challenges in grid operation [6,7]. Low-voltage grids are especially affected by this challenge, as they were historically designed to distribute energy to consumers, rather than to accommodate surplus generation from renewable energy sources [8].

Within this context, the integration of heat pumps (HPs) enables the direct use of renewable electricity for heat generation, forming a key link between the power and heating sectors and playing a determinant role in decarbonization strategies [9]. Coupled with intelligent control and thermal storage, they can align heat demand with renewable energy availability through load shifting, thereby enhancing both system flexibility and grid stability [10]. This integration transforms a traditionally demand-driven heat supply into an active component of a flexible, decarbonized energy system.

Especially large-scale centralized heat pumps are among the most effective solutions for multi-family houses (MFH) to enhance flexibility while meeting the demand for space heating and hot water generation [11,12]. This becomes particularly relevant in the case the MFH invested on a shared PV installation on the roof, enabling the building to produce energy and become an active participant in the electricity market.

However, the deployment of large-scale HPs faces several challenges, including technical barriers, social resistance, and market-related issues [13]. From a technical perspective, the primary challenges are associated with the modernization and digitalization of the heating sector, particularly the development of intelligent energy-management solutions. For instance, these control systems are designed to implement load shifting and peak shaving in heat pump operation, with the aim to achieve the maximization of self-consumption, minimization of costs, enhancement of thermal comfort, or reduction of environmental impact, among others [14]. On the social front, enabling users to actively interact with such control systems requires them to first acquire the necessary knowledge, and enhance engagement approaches. Social resistance is further compounded by limited technical expertise, system complexity, and a lack of practical experience and awareness among end users, installers, and engineers [13]. These knowledge gaps, coupled with low market transparency and unfavourable electricity-to-gas ratios, often strengthen the tendency to adopt traditional fossil fuel heating technologies [15]. Thus, developing easy-to-adopt and transparent control technologies is of prior importance for the further deployment of heat pumps. Moreover, emerging market instruments, such as dynamic pricing, interruptible tariffs, and participation in flexibility markets (e.g. balancing reserve, redispatch or local flexibility markets) create new incentives for flexible operation [16,17]. These mechanisms open new opportunities for HPs to respond to market signals and synchronize heat generation with renewable supply, potentially lowering operating costs while supporting system stability [18]. However, while dynamic tariffs are widely available, market penetration remains niche to date [19]. Access to balancing markets is potentially possible in Austria, but fulfilment of prequalification criteria is still a challenge for decentralized assets and operative connection requires intermediates, such as technical and commercial aggregators [20]. Technical aspects such as cycling behavior, minimum on/off times, and ramping limitations need to be considered in control algorithms and participation concepts to fully enable flexible and reliable operation of large-scale heat pumps [21].

Fischer and Madani reviewed frequently used control approaches for HP systems, their targets and applications [22]. They concluded that the choice of the control strategy is highly dependent on the specific building and integration approach, with model predictive controls (MPC) generally outperforming rule-based ones in thermal comfort maximization and operational costs minimization, as further confirmed by Q. Péan et al. [14]. This, however, leads to higher costs and increased system complexity. In another study, Fischer et al. investigated different control approaches for air-source HPs under constant and variable electricity prices, as well as PV production [23]. Their results show that MPC approaches can reduce annual operating costs (OPEX) by 6-11% with constant electricity prices and 6-16% with variable electricity prices, compared to 2-4% with rule-based approaches. Moreover, they demonstrated that the use of MPC can lead to increase in PV self-consumption up to 71%.

The aim of this study is to investigate the impact of different rule-based control strategies on large-scale HPs operation in residential buildings, in response to fluctuating renewable production, variable electricity prices and grid signals. The modelling of the building, its photovoltaic system, and heating plant model – including a centralized 60 kW heat pump and building's thermal as thermal energy storage (TES) – is conducted in the dynamic energy simulation software IDA ICE. A representative MFH is taken as reference building for the simulation (section 2.1). Yearly simulations are conducted for four distinct heat pump control scenarios (section 2.2), all considering HP operation only during the heating season. The investigated scenarios include: (A) "Base-case", (B) "PV-induced overconsumption", (C) "Variable electricity price", and (D) "Interruptible tariffs". A cost-driven analysis is performed to assess the economic benefits of different HP operations, complemented by a set of energy and thermal comfort KPIs, for further comparison (section 2.3).

2. Methodology

2.1. Reference building geometry and data

A multi-family house built in the early 1990s in Vienna is used as reference for the study (Fig. 1). The building underwent renovation in the mid-2010s. Being an energy-efficient building (energy class C) with reduced heating demand and low-temperature distribution systems, it provides favourable conditions for the use of a centralized heat pump. The implemented IDA ICE model focuses solely on the space heating system. Domestic hot water generation is not modelled, and it is assumed to be supplied by an independent unit.

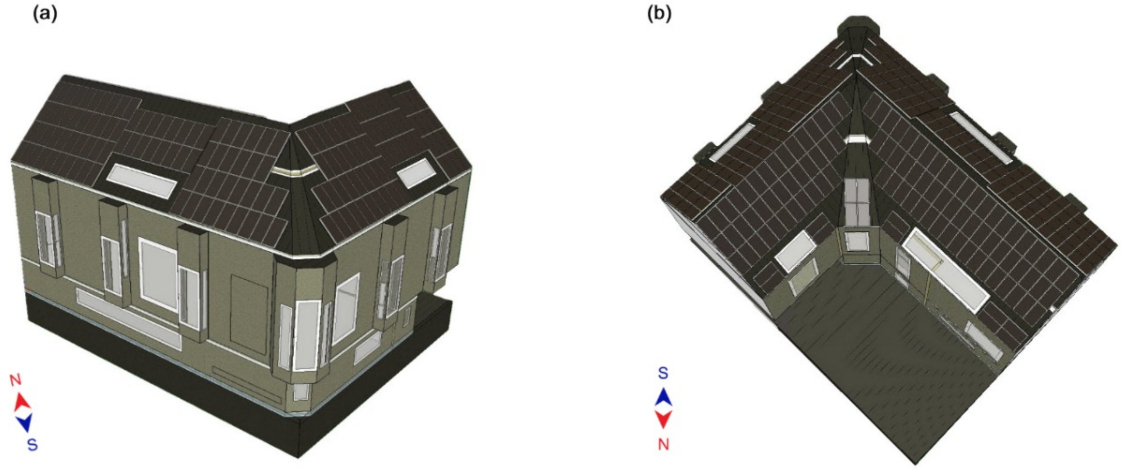

Figure 1. Lateral (a) and top (b) view of reference building simulated in IDA ICE.

The MFH contains 21 heated residential units, as well as non-heated communal areas (e.g., hallway, stairwell, garage, and ancillary storage spaces). Moreover, it is equipped with photovoltaic panels on the roof with total installed peak capacity of approximately 87.1 kWp.

To reduce computational efforts, adjacent rooms with similar functions (whether heated or unheated) are grouped and modelled as a single thermal zone. Moreover, fenestrations are combined into a single window within each thermal zone, while maintaining the same total surface area and frame-to-glass ratio. The U-values for the heated envelope range from 0.3–0.39 $\mathrm{W/m^2K}$, while the glazing U-value is up to 1.3 $\mathrm{W/m^2K}$.

The internal heat gain from occupants and equipment is calculated based on the following assumptions: an occupancy density of ~36 m²/person (typical for Viennese flats [24]), a defined occupant schedule during weekdays (0 from 08:00 to 15:00, 0.5 from 15:00 to 17:00, and 1 otherwise), and a full stay-at-home occupancy on weekends, which corresponds to the default occupancy schedule from IDA ICE for residential buildings. The energy consumption per apartment relative to equipment and lighting is modelled with 3000 kWh/year electricity use [25], assuming a 70% conversion factor to thermal load. The heating system consists of low-temperature radiators (45/38°C) with 22°C room temperature setpoint. Furthermore, no cooling system and mechanical ventilation are considered for the simulation.

2.2. Heat pump control scenarios

The reference MFH is equipped with one centralised large-scale ground-source heat pump of 60 kW thermal capacity and a COP of 4.2. The heat pump capacity is sized to meet the building annual peak heating load, with an additional safety margin of approximately 20%. Additionally, the heat pump is connected to a 1 m^3 hot water tank, used as hydraulic buffer and not for storage purposes. The building's thermal mass is used as the primary storage for the MFH. The heat pump operation is simulated under fluctuating renewable electricity production from the PV system installed on the roof, as well as variable electricity prices and grid signals. Thus, four distinct control strategies are developed and presented in Table 1.

Notably, across all scenarios, the electricity generated by the PV system is always self-consumed, provided there is a demand for it. Moreover, when PV production exceeds the heat pump load (PV surplus), the energy is sold to the grid assuming the day-ahead price as feed-in tariff minus the according grid fees.

Table 1. Description and main differences between heat pump control scenarios: (A) "Base-case", (B) "PV-induced overconsumption", (C) "Variable electricity price", (D) "Interruptible tariffs".

Heat pump control scenarios	Brief description and goal	Supply temperature shift	Room temperature shift
(A) Base-case	Standard control. Heat pump load not modified.	No	No
(B) PV-induced overconsumption	PV-ruled scenario. Goal: Reduce OPEX by increasing self-consumption from PV-produced electricity.	Yes, according to overconsumption rule (Fig. 5) $T_{supply-shift:}$ $0\ K \leq \Delta T \leq 5\ K$	Yes $T_{room-shift:}$ $0\ K \leq \Delta T \leq 5\ K$
(C) Variable electricity price	Electricity price-ruled scenario. Goal: Reduce OPEX by profiting from negative electricity prices (Fig. 6).	Yes, according to price rule (Fig. 8) $T_{supply-shift:}$ 45°C	Yes $T_{room-shift:}$ $0\ K \leq \Delta T \leq 5\ K$
(D) Interruptible tariffs	Grid tariffs-ruled scenario. Goal: Reduce OPEX by profiting from incentivized grid tariffs.	No	No

In Scenario (B), the ratio of PV self-consumption is increased by adjusting the heat pump operation, i.e., shifting the supply temperature by up to +5K. Moreover, the room setpoint temperature is also shifted by +5K to accommodate and store this additional energy within the building's thermal mass.

The supply and room temperatures shifts follow Eq. 1, and are calculated from the Outdoor Temperature Compensation Curve (OTCC) setpoint based on the outdoor temperature T_{out} and the PI controller output u_{PI} (0 to 1):

$$T_{shift} = T_{OTCC}(T_{out}) + u_{PI} \cdot 5\ K,\ \ u_{PI} \in [0,1] \tag{1}$$

In Scenario (C), the heat pump operation is adjusted based on the Day-Ahead (DA) variable electricity prices. Specifically, during periods of negative price events, the heat pump supply temperature setpoint and the room temperature setpoint are increased by 5 K to minimize operating costs. It should be noted that, in both Scenarios (B) and (C), a +5 K temperature setpoint shift does not necessarily violate thermal comfort. In fact, any transient overheating may still remain within comfort limits due to building thermal dynamics, system capacity limits, and the limited duration of the control action.

Finally, in Scenario (D), the heat pump is shut down in periods when the grid operator interrupts energy supply to reduce consumption peaks. In this case the interruptible tariff scheme applies, which results in reduced grid fees. A summary of electricity costs and grid tariffs is provided in Table 2.

Table 2. Electricity costs (regular and incentivized) and feed-in price for the four investigated scenarios. Assumption: heat pump is connected on LV grid level 7 in Vienna.

Buy/Sell scenario	Description	Electricity price [ct/kWh]	Grid fee [ct/kWh]	Final electricity cost/feed-in including VAT [ct/kWh]
Buy electricity tariff scheme for scenarios (A), (B), (C)	Regular electricity cost	Day-ahead electricity price	Sum between grid usage fee (5.3 ct/kWh) and grid loss fee (0.866 ct/kWh)	$Eq. 2: El_{cost} = (DA_{price} + 6.17) \cdot 1.2$
Buy electricity tariff scheme for scenario (D)	Electricity cost under incentivized interruptible grid tariff scheme	Day-ahead electricity price	Sum between reduced grid usage fee (2.88 ct/kWh) and grid loss fee (0,866 ct/kWh)	$Eq. 3: El_{cost_D} = (DA_{price} + 3.75) \cdot 1.2$
Sell electricity tariff scheme for scenarios (A), (B), (C), (D)	Regular electricity feed-in price	Day-ahead electricity price	Grid loss fee (0.468 ct/kWh)	$Eq. 4: El_{feed-in} = DA_{price} - 0.468$

Electricity prices affect HP operation exclusively in Scenario (C). For the calculation of economic KPIs in all scenarios, the electricity consumed from the grid was valued with the price on the Day-Ahead Market to guarantee comparability. This approach reflects at least the minimum costs a supplier would need to cover under a fixed-tariff scheme. Additional grid fees were as well considered in the evaluation (see Table 2).

2.2.1. Scenario (A): Base-case

In this scenario, the building's energy demand is primarily met by locally produced energy from the PV system, whenever generation is available (Fig. 2). However, if the PV system cannot fully meet the required HP load, the remaining energy is purchased from the grid. Conversely, when PV production exceeds the heat pump load, the surplus energy is sold to the grid. The implementation of the control scenario in IDA ICE is illustrated in Fig. 3.

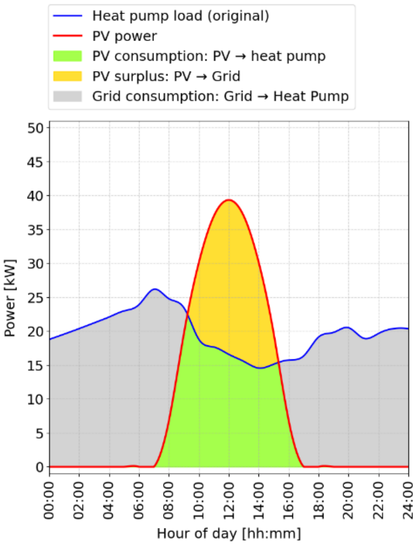

Figure 2. Schematic of Scenario (A).

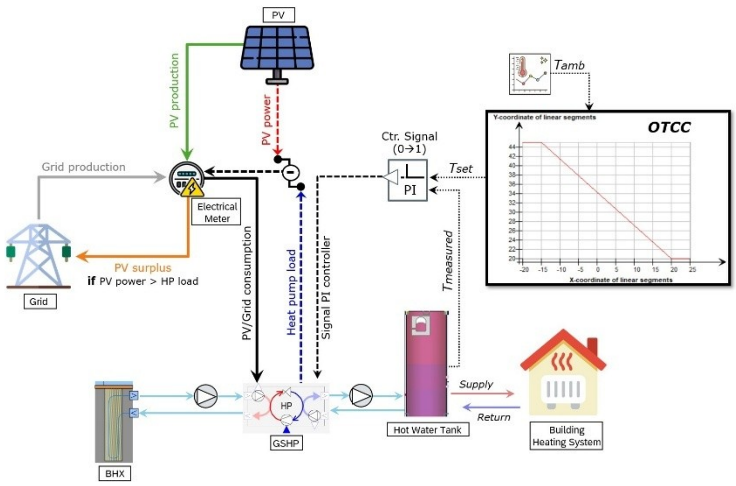

Figure 3. Sketch of control strategy implemented in IDA ICE for Scenario (A).

It must be noted that, in the IDA ICE model, the heat pump's control signal is modulated based on the temperature measured in the hot-water storage tank, which follows a linear control law relating the heating supply temperature to the ambient air temperature. Therefore, the controller does not directly regulate the heat pump operation, but only indirectly, through the storage tank setpoint.

2.2.2. Scenario (B): PV-induced overconsumption

The main objective of this scenario is to reduce OPEX by increasing self-consumption of PV-produced energy by storing heat in advance when free renewable electricity is available, and reduce grid consumption at later points of time. This is achieved by artificially modifying the heat pump load, increasing the secondary side flow temperature and the room thermostat setting with maximum temperature shifts of +5K.

In case of PV electricity production, the heat pump load is shifted to accommodate the available extra-energy and store it within the building's thermal mass, until the room setpoint conditions are reached, i.e. the indoor temperature reaches 27 °C (22°C + 5 °C). This process involves continuous monitoring of the PV output and comparison with the instantaneous heat pump consumption. Finally, when the indoor temperature reaches the (shifted) setpoint value, all the extra-energy is considered as stored, and the heating supply and room setpoint temperatures are set back to their original value. Moreover, any remaining surplus energy is fed into the grid. Fig. 4 illustrates a representative day of operation under this control strategy, while Fig. 5 provides a schematic summary of its implementation in IDA ICE.

It should be noted that the curves in Fig. 4 are artificial profiles and introduced solely to illustrate the control logic. Consequently, they are not intended to capture the true dynamic response of the system or any rebound phenomena. For instance, under real operating conditions the heat pump load would typically decrease following overheating, and only later return to the original load (blue curve).

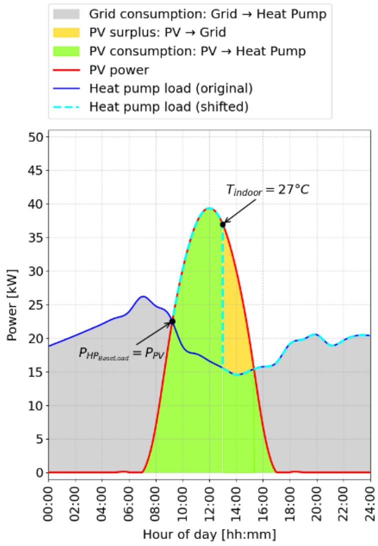

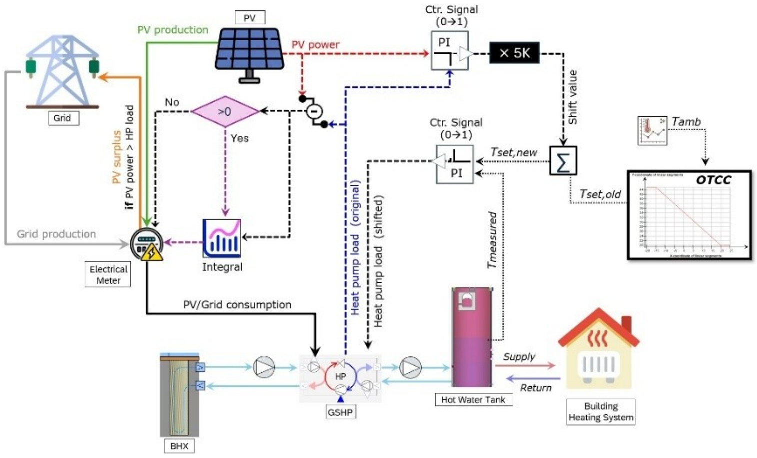

Figure 4. Schematic of Scenario (B).

Figure 5. Sketch of control strategy implemented in IDA ICE for Scenario (B).

2.2.3. Scenario (C): Variable electricity price

The objective of this scenario is to minimize OPEX by preheating the building during periods of negative electricity prices. The variable day-ahead electricity prices from the heating season of 2024 [26], here defined between the 1st of January and the 15th of April, and between the 15th of October and the 31st of December, are used for the purpose of the investigation (see Fig. 6). Thus, whenever the electricity prices are negative, the heat pump is forced to work at maximum load by shifting the supply temperature to a constant value of 45°C. In all other cases, the heat pump load is kept unvaried. Notably, this occurrence corresponds to approximately the 2nd percentile of the total DA electricity price dataset, i.e., only a limited number of hours during the year. Thus, thermal comfort is mostly ensured, and no severe overheating is expected, while enabling more profitable cost savings.

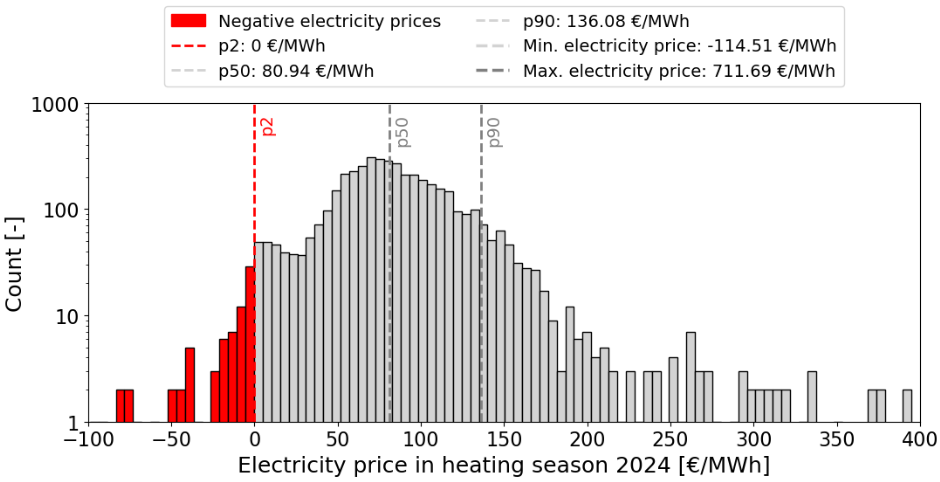

Figure 6. Supply temperature shifts according to negative electricity prices in heating season 2024. Percentile values for p2, p50 and p90 are showed as reference.

Fig. 7 illustrates the application of this scenario for a representative day (artificial profiles). The heat pump load is modulated in response to the electricity prices (cyan dotted curve). Thus, when the electricity price falls below 0 €/MWh, a shift is applied to the heat pump supply temperature, resulting in an increased load and temporary overheating of the building. It should be noted that, in reality, the heat pump load does not increase instantaneously, but gradually due to system dynamics and control behavior. In all other cases, the heat pump load remains unchanged, corresponding to the original profile (solid blue curve). The modified heat pump load (cyan curve) is supplied either by PV generation, when available, or purchased from the grid. Any surplus electricity is sold to the grid. The corresponding configuration of this control strategy in IDA ICE is illustrated in Fig. 8.

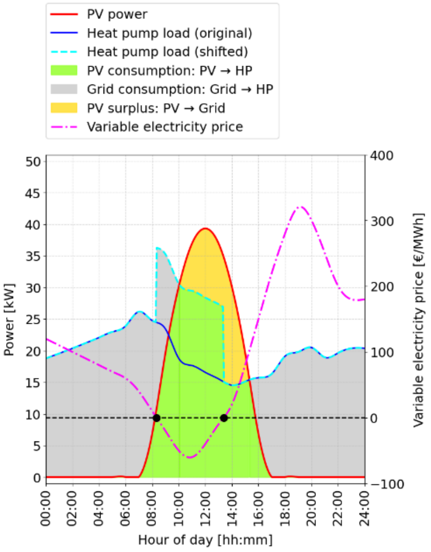

Figure 7. Schematic of Scenario (C).

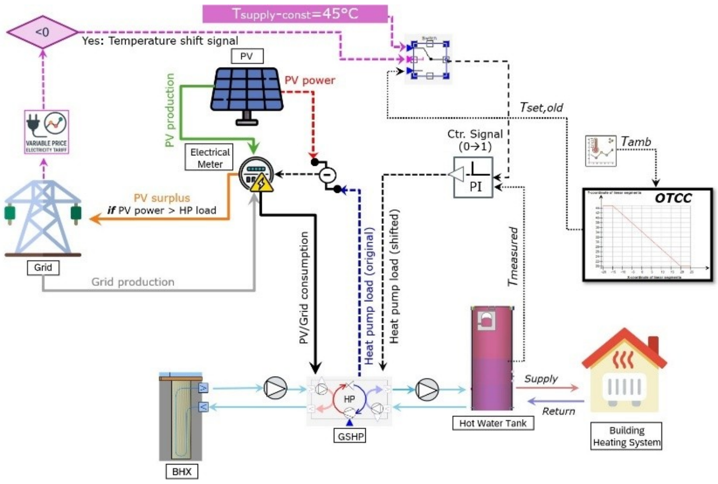

Figure 8. Sketch of control strategy implemented in IDA ICE for Scenario (C).

Notably, Fig. 7 does not capture the true system dynamic, and the represented profiles only illustrate the implemented control mechanism. For instance, they neglect the typical decrease in HP load following the overheating triggered by negative electricity prices.

2.2.4. Scenario (D): Interruptible tariffs

This scenario focuses on the adaptability of heat pump operation under interruptible grid tariffs. For instance, operation may be curtailed during peak hours to mitigate grid congestion. In such cases, it becomes necessary to shut down the heat pump operation in order to enhance grid stability, while economically benefitting from reduced grid tariffs (see Table 2).

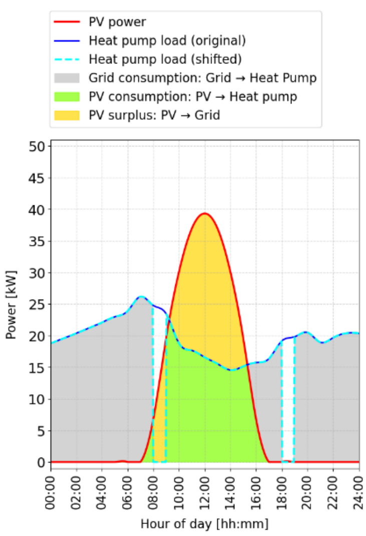

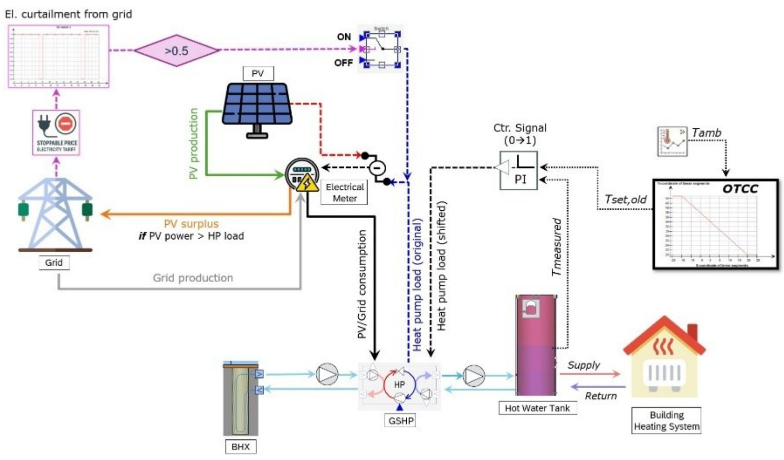

Figure 9. Schematic of Scenario (D).

Figure 10. Sketch of control strategy implemented in IDA ICE for Scenario (D).

In the model implemented in IDA ICE, two one-hour planned power outages are scheduled between 8:00-9:00 and 18:00-19:00 every day. An exemplary operation of the system is provided in Fig. 9 (artificially generated power profiles), while its implementation in IDA ICE is schematically shown in Fig. 10. It should be considered that, under real operating conditions, additional rebound effects are expected following the heat pump shutdown periods, such as increased energy consumption to compensate for the preceding drop in indoor temperature.

2.3. Key Performance Indicators

The analysed scenarios are compared based on the KPIs listed in Table 3, which are categorized into energy-related, economic, and thermal comfort indicators.

Table 3. Key performance indicators.

KPI	Category	Definition	Calculation	Unit
COP	Energy	Coefficient of Performance: Ratio between the heat output (Q_{HP}, kWh) and the electrical input (E_{HP}, kWh) for the heat pump during operation, excluding parasitic loads. Q_{HP} and E_{HP} are direct outputs from IDA ICE.	Eq. 5: $COP = Q_{HP}/E_{HP}$	-
SSR	Energy	Self-Sufficiency Ratio: Share of the heat pump electrical energy demand (E_{HP}, kWh) met by PV self-production ($E_{PV_{self}}$, kWh) during the heating season.	Eq. 6: $SSR = (E_{PV_{self}}/E_{HP}) \cdot 100$	%
$E_{surplus}$	Energy	Share of total PV production (E_{PV}, kWh) that is purchased by the grid ($E_{PV_{sold}}$, kWh).	Eq. 7: $E_{surplus} = (E_{PV_{sold}}/E_{PV}) \cdot 100$	%
$OPEX$	Economic	Operational Expenditure for heat pump: Sum of the cost of electricity purchased from the grid and the lost revenues from the self-produced PV electricity used to run the heat pump instead of being sold to the grid.	Eq. 8: $OPEX = \left(E_{HP} - E_{PV_{Self}}\right) \cdot El_{cost} + E_{PV_{Self}} \cdot E_{feed-in}$	€
$Savings$	Economic	Seasonal savings compared to base-case scenario.	Eq. 9: $Savings_{Scenario} = OPEX_{Base-case} - OPEX_{Scenario}$	€
$Savings_{\%}$	Economic	Seasonal savings compared to base-case scenario (percentage value).	Eq. 10: $Savings_{\%} = (Savings_{Scenario}/OPEX_{Base-case}) \cdot 100$	%
$Cost$	Economic	Actual cost paid by the consumer, calculated as the difference between the costs for electricity from the grid and revenue coming from sold electricity to the grid.	Eq. 11: $Cost_{Scenario} = \left(E_{HP} - E_{PV_{Self}}\right) \cdot El_{cost} - (E_{PV_{sold}} \cdot El_{feed-in})$	€
$h_{comfort}$	Thermal comfort	Number of hours during the heating season (15th Oct. – 15th April) where indoor temperature is within comfort band (defined between 20 – 24°C, according to ISO 16798-1 [27], Cat. II).	Eq. 12: $h_{comfort} = \sum_{i=1}^{h=4380} 1 \cdot \{T_{indoor}(i) \in [20,24]\}$	h

3. Results and Discussion

Figure 11 shows the seasonal energy flows in MWh during the heating season across the four investigated scenario, as well as the Self-Sufficiency Ratio (SSR) and the ratio of exported PV electricity ($E_{surplus}$). The exact values are additionally presented in Table 4, where the heat pump load (E_{HP}) is reported as the sum of PV self-produced electricity ($E_{PV_{Self}}$) and the energy purchased from the grid.

As specified in Table 1, the goal of the control strategy in Scenario (B) is to achieve a reduction in OPEX by increasing self-consumption from PV-produced electricity, and decreasing the amount of grid electricity purchased during evening time, when a peak in electricity consumption is usually registered at grid level. As noticeable, this objective is fulfilled, as this scenario exhibits the highest SSR (63%), with a total of 9.28 MWh of self-produced and consumed PV electricity out of 14.64 MWh HP load. As a direct consequence, the amount of electricity purchased from the grid is the lowest (5.36 MWh) among all scenarios, as well as the energy sold to the grid (10.91 MWh). Moreover, since the supply and room setpoint temperatures are shifted up by maximum 5K, overheating of the building's thermal mass occurs. This excess heat helps storing energy during periods of excess PV production; however, it also leads to thermal discomfort, as further evidenced in Fig. 12. In this scenario, indoor temperatures exceed 24°C for approximately 18% of the heating season, compared to less than 0.5% in the base-case scenario. Results from economic calculations are shown in Table 5. As visible, this scenario is 7.6% more profitable than the base-case, primarily due to the reduced consumption of grid electricity, thanks to both the higher PV self-consumption and the lower electricity demand at later times resulting from overheating.

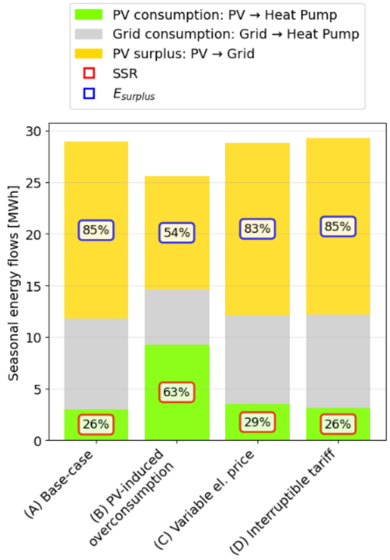

Table 4. Seasonal energy flows for HP, PV and grid in the four investigated scenarios.

Scenario	HP load E_{HP} [MWh]	PV consumption $E_{PV_{Self}}$ [MWh]	PV Surplus $E_{PV_{sold}}$ [MWh]	Grid consumption [MWh]
(A)	11.75	3.01	17.18	8.74
(B)	14.64	9.28	10.91	5.36
(C)	12.13	3.50	16.69	8.63
(D)	12.16	3.11	17.08	9.05

Figure 11. Seasonal energy flows. SSR is expressed in percentage within the PV consumption green bars ($E_{PV_{self}}$). The ratio of exported PV electricity is expressed in percentage within the PV surplus yellow bars ($E_{PV_{sold}}$). The purchased energy is shown in the grey bars.

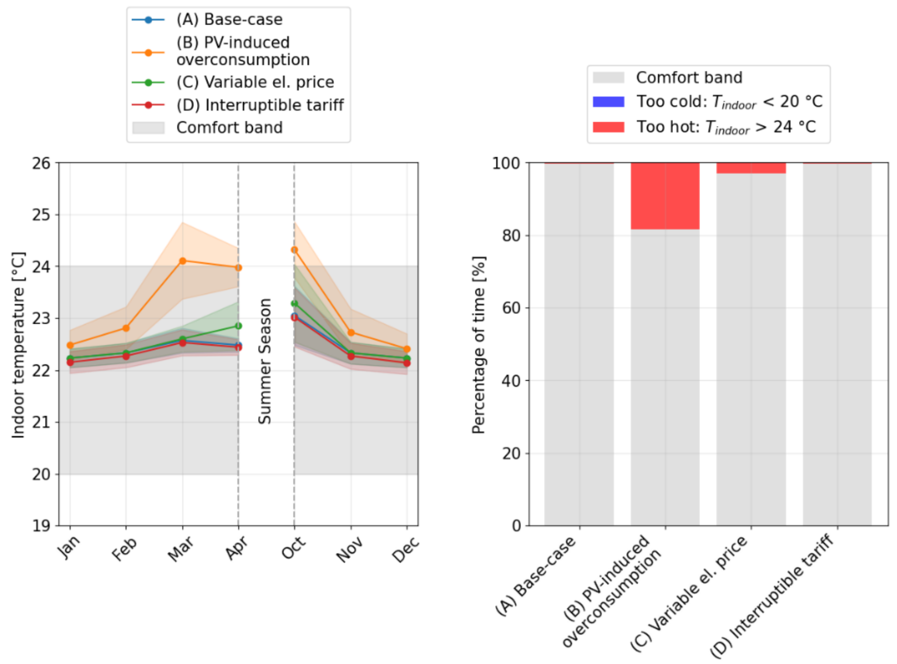

Figure 12. Monthly average mean indoor temperatures for the four scenarios including range for standard deviation (left); Percentage of time where thermal comfort is met during heating season (right). Thermal comfort band defined between 20 – 24°C (Category II ISO 16798-1; PPD < 10%).

The objective of Scenario (C) is to reduce OPEX for the heat pump by benefitting from the negative electricity prices and forcing the heat pump to work at higher load during these periods of time. Notably, these occurrences might take place with or without simultaneous PV generation. Consequently, this strategy shows only limited benefits in terms of SSR relative to the base-case. However, it allows thermal storage in the building thermal mass (overheating), while achieving thermal comfort in 97% of the times (Fig. 12). From an economic savings perspective, this scenario is slightly more profitable compared to the base-case. However, the benefit is limited, with savings below 2%, as negative-price hours represent only the 2nd percentile of the overall day-ahead electricity price dataset.

Finally, the objective of Scenario (D) is to take advantage of the incentivized grid tariffs and shutdown the heat pump in response to the curtailment signals coming from the grid. From an economic perspective, this scenario ranks the most profitable, thanks to the reduced grid tariffs for electricity purchases (Table 2), resulting in savings of 10.7% during the heating season compared to the base-case scenario. Moreover, from a thermal comfort perspective, this scenario performs as good as the base-case, with the indoor temperature falling within the comfort band >99.7% of the times. It could be concluded that, due to the system dynamics, the heat pump shutdown does not severely impact thermal comfort, and even if a drop in room temperature might take place during the curtailment periods, this never falls below 20°C and is compensated shortly after by increased HP operation. It is worth noticing that in all scenarios the HP load (sum of grey and green bars in Fig. 11) exceeds that of the base-case. Scenario (B) shows the largest deviation, driven by substantial overheating, e.g., higher HP operation from excess PV production. In Scenario (C), this is a direct consequence of the increased HP operation during negative electricity price occurrences. In Scenario (D), the effect is attributed to the additional energy required to restore the indoor temperature setpoint after the HP shutdown.

Table 5. Economic KPIs.

Scenario	OPEX[1] [€]	Savings [€]	Savings $_{\%}$ [%]	Actual cost [€] (incl. HP costs and total PV revenues)
(A) Base-case	1929	-	-	592
(B) PV- induced overconsumption	1782	147	7.6	444
(C) Variable el. price	1895	34	1.8	557
(D) Interruptible tariff	1722	207	10.7	384

By analysing key indicators related to the operation of the HP, namely the condenser heat and the COP, further insights can be drawn regarding its load and operational efficiency (see Fig. 13).

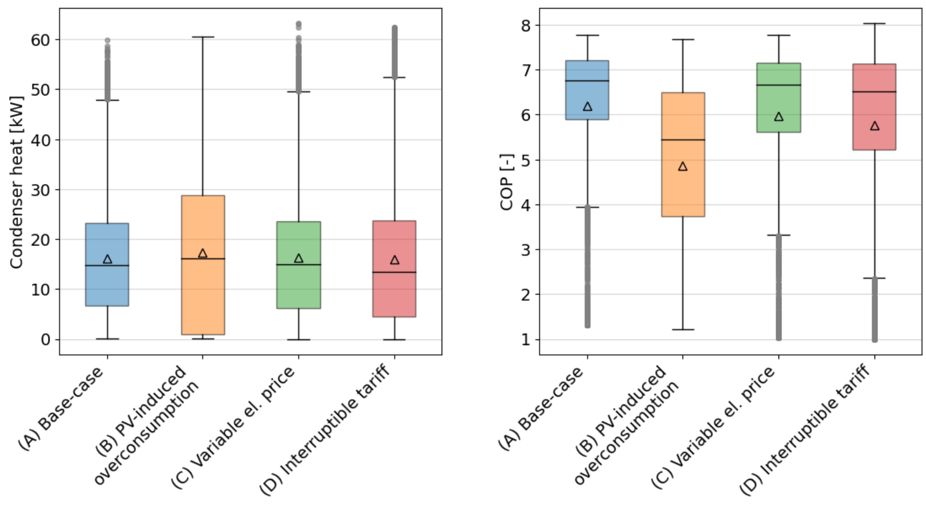

Figure 13. Heat pump condenser heat (left) and Coefficient of Performance COP (right) during the heating season for the four scenarios, based on simulation hourly-average profile records. The mean values are indicated by triangles, and the median values by horizontal lines.

As anticipated, in all scenarios where the heat pump load is actively shifted to achieve overheating – scenarios (B) and (C) – the maximum amount of heat delivered by the heat pump is higher than the base-case. Moreover, this also occurs for Scenario (D), since right after its shutdown the heat pump operation will automatically adjust to work at higher loads to compensate the decrease in indoor temperature. However, the mean values of the condenser heat are relatively comparable in all the scenarios, around 16 kWh. It is important to note that

1 Includes lost revenues from PV electricity used for self-consumption.

shifts in the heat pump load often come at the expense of system performance, as operating under shifted temperature setpoints typically increases energy use and reduces the system COP. Moreover, the heat pump may be forced to operate during periods when the temperature lift between the source and sink is higher, in order to meet other economic and flexibility objectives. Thus, scenarios (C) and (D) achieve comparable COPs of 5.8–6.0, whereas scenario (B), with more significant overheating, shows the lowest mean COP (4.9). The best performing scenario is the base-case, with average COP of 6.2 and more consistent HP operation.

4. Conclusions

This study presents an initial approach to comparing the economic profitability, system efficiency, and thermal comfort of a large-scale residential heat pump under four different rule-based control strategies. The analysis shows that Scenario (D) is the most economically profitable, primarily due to reduced grid fees. It achieves a seasonal OPEX reduction of 10.7% relative to the base-case scenario, with high level of thermal comfort (met >99.7% of the times). Furthermore, Scenario (B) records the highest SSR of 63%, thus indirectly contributing to grid stability by preventing overload during peak hours. However, increasing the heating supply temperature by +5K proved to be an excessive setpoint for the system, which not only leads to overheating of the building's thermal mass but also determines a rise in the indoor temperature above 24°C for 18% of the times. Finally, the incremental economic value of Scenario (C) is marginal, with seasonal savings remaining below 2%, as negative-price hours represent only the 2nd percentile of the overall day-ahead electricity price dataset. Moreover, in all scenarios a shift in the heat pump load often come at the expense of system performance, with the base-case scenario resulting as the most efficient solution with average COP of 6.2. Deviations in COP between the scenarios are attributable to the supply temperature and room temperature setpoint shifts, resulting in higher electricity consumption and a lower HP performance. To conclude, the authors acknowledge that this initial analysis is insufficient to draw definitive conclusions about the optimal operation of large-scale heat pumps, as the strategies applied do not specifically optimize any energy, economic or thermal comfort function, or a combination of those. Future research should focus on the development of scenarios that combine multiple KPIs-optimization, along with the development of MPC strategies to accurately predict the heat pump load and adjust its operation accordingly. Moreover, future work should examine how domestic hot water tank storage size influences the overall system performance, particularly when operated as TES.

Acknowledgements

This project WPOpt4Grid (FFG #920939) is supported with the funds from the Climate and Energy Fund and implemented in the framework of the Energieforschungsprogramm 2024 (KLIEN).

References

[1] IEA. The Future of Heat Pumps 2022. https://doi.org/10.1787/2bd71107-en.
[2] Meiers J, Ortleb M, Jonas D, Tadayon L, Frey G. Control strategies for heat pumps in a residential area under consideration of system operator benefits and grid stability. Energy and Buildings 2025;332:115442. https://doi.org/10.1016/j.enbuild.2025.115442.
[3] Parra-Domínguez J, Sánchez E, Ordóñez Á. The Prosumer: A Systematic Review of the New Paradigm in Energy and Sustainable Development. Sustainability 2023;15:10552. https://doi.org/10.3390/su151310552.
[4] Stefan M, Šipetić M, Giordano F, Korner C, Ray Payonga L, Emiliani V, et al. Optimizing renewable energy communities through ontology-driven energy management systems. IET Conf Proc 2025;2025:1933–7. https://doi.org/10.1049/icp.2025.1962.
[5] Eibl G, Radovanovic D, Reihs D, Kapeller R, Stefan M, Reichl J. Assessment of the influence of renewable energy communities on future scenarios of the distribution grid. IET Conf Proc 2025;2024:329–32. https://doi.org/10.1049/icp.2024.2051.
[6] Petinrin JO, Shaabanb M. Impact of renewable generation on voltage control in distribution systems. Renewable and Sustainable Energy Reviews 2016;65:770–83. https://doi.org/10.1016/j.rser.2016.06.073.
[7] Shafiullah M, Ahmed SD, Al-Sulaiman FA. Grid Integration Challenges and Solution Strategies for Solar PV Systems: A Review. IEEE Access 2022;10:52233–57. https://doi.org/10.1109/ACCESS.2022.3174555.
[8] Guo R, Meunier S, Protopapadaki C, Saelens D. A review of European low-voltage distribution

networks. Renewable and Sustainable Energy Reviews 2023;173:113056. https://doi.org/10.1016/j.rser.2022.113056.
[9] Siddique MB, Keles D, Scheller F, Nielsen PS. Dispatch strategies for large-scale heat pump based district heating under high renewable share and risk-aversion: A multistage stochastic optimization approach. Energy Economics 2024;136:107764. https://doi.org/10.1016/j.eneco.2024.107764.
[10] Schöniger F, Mascherbauer P, Resch G, Kranzl L, Haas R. The potential of decentral heat pumps as flexibility option for decarbonised energy systems. Energy Efficiency 2024;17:26. https://doi.org/10.1007/s12053-024-10206-z.
[11] Fraga C, Hollmuller P, Schneider S, Lachal B. Heat pump systems for multifamily buildings: Potential and constraints of several heat sources for diverse building demands. Applied Energy 2018;225:1033–53. https://doi.org/10.1016/j.apenergy.2018.05.004.
[12] Miara, M. (ed.). Annex 50 Final Report "Heat Pumps in Multi-Family Buildings for Space Heating and Domestic Hot Water". Report No HPT-AN50-1 2022.
[13] Schlosser F, Jesper M, Vogelsang J, Walmsley TG, Arpagaus C, Hesselbach J. Large-scale heat pumps: Applications, performance, economic feasibility and industrial integration. Renewable and Sustainable Energy Reviews 2020;133:110219. https://doi.org/10.1016/j.rser.2020.110219.
[14] Péan TQ, Salom J, Costa-Castelló R. Review of control strategies for improving the energy flexibility provided by heat pump systems in buildings. Journal of Process Control 2019;74:35–49. https://doi.org/10.1016/j.jprocont.2018.03.006.
[15] Jesper M, Schlosser F, Pag F, Walmsley TG, Schmitt B, Vajen K. Large-scale heat pumps: Uptake and performance modelling of market-available devices. Renewable and Sustainable Energy Reviews 2021;137:110646. https://doi.org/10.1016/j.rser.2020.110646.
[16] Cano-Martínez J, Quijano-López A, Fuster-Roig V. A Scoping Review of Flexibility Markets in the Power Sector: Models, Mechanisms, and Business Perspectives. Energies 2025;18:5213. https://doi.org/10.3390/en18195213.
[17] Faruqui A, Sergici S. HOUSEHOLD RESPONSE TO DYNAMIC PRICING OF ELECTRICITY—A SURVEY OF THE EXPERIMENTAL EVIDENCE n.d.
[18] Langner F, Kovačević J, Zwickel P, Dengiz T, Frahm M, Waczowicz S, et al. Coordinated price-based control of modulating heat pumps for practical demand response and peak shaving in building clusters. Energy and Buildings 2024;324:114940. https://doi.org/10.1016/j.enbuild.2024.114940.
[19] Numminen S, Jalas M, Ruggiero S, Värä A. Shifting toward dynamic pricing of electricity: What did we learn from the 2021–2024 energy crises? Smart Energy 2025;20:100210. https://doi.org/10.1016/j.segy.2025.100210.
[20] Poplavskaya K, De Vries L. Distributed energy resources and the organized balancing market: A symbiosis yet? Case of three European balancing markets. Energy Policy 2019;126:264–76. https://doi.org/10.1016/j.enpol.2018.11.009.
[21] Evens M, Arteconi A. Influence of internal control simplifications in heat pump system modelling for energy flexibility evaluations, 2021. https://doi.org/10.26868/25222708.2021.30214.
[22] Fischer D, Madani H. On heat pumps in smart grids: A review. Renewable and Sustainable Energy Reviews 2017;70:342–57. https://doi.org/10.1016/j.rser.2016.11.182.
[23] Fischer D, Bernhardt J, Madani H, Wittwer C. Comparison of control approaches for variable speed air source heat pumps considering time variable electricity prices and PV. Applied Energy 2017;204:93–105. https://doi.org/10.1016/j.apenergy.2017.06.110.
[24] Stadt Wien. Vienna in Figures 2024 n.d. ISSN 1028-0723. statistik.wien.gv.at.
[25] Energiebericht der Stadt Wien / Medieninhaber und Herausgeber: Magistrat der Stadt Wien, Magistratsabteilung 20 - Energieplanung. Wien : Magistrat der Stadt Wien, Magistratsabteilung 20 - Energieplanung, 2025- : (2025). Wienbibliothek im Rathaus, https://resolver.obvsg.at/urn:nbn:at:AT-WBR-1933776 / Urheberrechtsschutz (InC 1.0). 2025.
[26] European Wholesale Electricity Price Data n.d. https://ember-energy.org/data/european-wholesale-electricity-price-data/.
[27] European Committee for Standardization. EN 16798-2 TR:2014 (E): Energy performance of buildings – Ventilation for buildings – Part 2: Indoor environmental input parameters for design and assessment of energy performance of buildings. CEN. 2014.